Spin Reorientation at the Antiferromagnetic NiO(001) Surface in Response to an Adjacent Ferromagnet

H. Ohldag,[1,2,3] A. Scholl,[2] F. Nolting,[1,2] S. Anders,[2] F. U. Hillebrecht,[4] and J. Stöhr[1]
[1]*Stanford Synchrotron Radiation Laboratory, P.O. Box 20450, Stanford, California 94309*
[2]*Advanced Light Source, Lawrence Berkeley National Laboratory, 1 Cyclotron Road, Berkeley, California 94720*
[3]*Institut für Angewandte Physik, Universität Düsseldorf, Universitätsstrasse 1, 40225 Düsseldorf, Germany*
[4]*Max Planck Institut für Mikrostrukturphysik, Weinberg 2, 06120 Halle, Germany*
(Received 22 September 2000)

Polarization dependent x-ray photoemission electron microscopy was used to investigate the spin structure near the surface of an antiferromagnetic NiO(001) single crystal in response to the deposition of a thin ferromagnetic Co film. For the cleaved NiO surface we observe only a subset of bulklike antiferromagnetic domains which is attributed to minimization of dipolar energies. Upon Co deposition a spin reorientation near the NiO interface occurs, with the antiferromagnetic spins rotating in plane, parallel to the spins of the Co layer. Our results demonstrate that the spin configuration in an antiferromagnet near its interface with a ferromagnet may significantly deviate from that in the bulk antiferromagnet.

DOI: 10.1103/PhysRevLett.86.2878 PACS numbers: 75.70.–i, 75.70.Rf, 75.50.Ee, 78.20.Ls

The macroscopic *exchange bias* effect, i.e., the unidirectional exchange coupling between an antiferromagnet (AFM) and a ferromagnet (FM), that appears when an AFM-FM sandwich is grown or heated in a magnetic field, has been the subject of extensive studies because of its technological relevance and lack of scientific understanding [1,2]. In light of the difficulty of determining the AFM structure close to the FM interface most models have assumed that the antiferromagnetic spin structure in the bulk, which in most cases is known from neutron diffraction, extends all the way to the interface. An example is the recent study of the Fe/NiO(001) system [3] where a bulklike NiO(001) domain structure was assumed to model the AFM-FM coupling.

During the last year, progress made with imaging methods based on variable polarization x rays has allowed the observation of the microscopic spin structure on both sides of an AFM-FM interface [4]. Studies of the $Co/LaFeO_3(100)$ system convincingly showed the direct correlation of the antiferromagnetic and ferromagnetic spin structure near the interface and the existence of local exchange bias, domain by domain. However, because of the complex antiferromagnetic structure of twinned epitaxial $LaFeO_3(100)$ the three-dimensional correlation between the ferromagnetic and antiferromagnetic spin directions could not be determined. Using the well-studied antiferromagnet NiO, coupled to either a thin Fe or Co layer, we are able to experimentally determine here the relative alignment of the antiferromagnetic and ferromagnetic spin systems. We show that the magnetic spins near the surface of a NiO(001) single crystal and those in a thin film of Co or Fe deposited on top align perfectly parallel to each other. Our finding is in complete contrast to the recent conclusions of Matsuyama *et al.* [3] for the same system, who assumed a bulklike NiO spin structure at the interface. Rather, our results reveal a reorientation of the antiferromagnetic spins near the NiO(001) surface upon deposition of the ferromagnetic film. More importantly, they provide clear experimental evidence that symmetry breaking at surfaces and interfaces will in general lead to spin reorientation effects in antiferromagnets.

The x-ray photoemission electron microscopy (XPEEM) experiments were performed on beam line 7.3.1.1 at the Advanced Light Source using the PEEM2 microscope [5]. The microscope has a lateral resolution of about 50 nm when used for magnetic imaging. The depth sensitivity is determined by the escape depth of the secondary electrons. Because of the elemental specificity of the x-ray absorption process we can distinguish the signal from layers with different elemental composition with a $1/e$ probing depth of about 2 nm for each layer [6]. The bending magnet x-ray source and the spherical grating monochromator provide monochromatic x rays with an energy resolution of 0.6 eV at 850 eV and adjustable polarization ranging from linear ($\sim$90%) to left- or right-handed circular ($\sim$80%). Figure 1 shows the experimental geometry. X rays are incident on the sample at an angle $\theta = 30°$ from the surface.

For x-ray magnetic *linear* dichroism (XMLD) measurements we typically use linearly polarized x rays with the electric field vector $\vec{\mathbf{E}}$ parallel to the sample surface. In all XMLD measurements we use the experimentally observed fact that the intensity of the higher energy peak at the Ni L_2-edge is at a maximum when the $\vec{\mathbf{E}}$ vector is aligned parallel to the antiferromagnetic axis [7,8]. By rotating the sample about the surface normal we can change the azimuthal angle ϕ between the in-plane $\vec{\mathbf{E}}_{\parallel}$ vector and the [100] direction of the NiO crystal. This allows us to determine the in-plane orientation of the antiferromagnetic axis. We cannot rotate the direction of the linearly polarized x rays but we can obtain out-of-plane XMLD sensitivity by using circularly polarized x rays. In this case

 0031-9007/01/86(13)/2878(4)$15.00

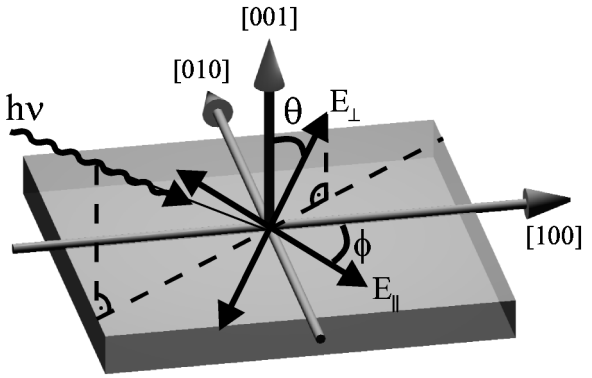

FIG. 1. Experimental geometry. The x rays are incident at an angle $\theta = 30°$ from the surface and the elliptical polarization may in general be divided into an in-plane $\vec{\mathbf{E}}_{\parallel}$ and out-of-plane $\vec{\mathbf{E}}_{\perp}$ component. $\vec{\mathbf{E}}_{\perp}$ is inclined by $\theta = 30°$ from the surface normal and $\vec{\mathbf{E}}_{\parallel}$ is oriented at an angle ϕ from the in-plane [100] axis.

the handedness of the x rays is irrelevant since only the relative sizes of the in-plane ($\vec{\mathbf{E}}_{\parallel}$) and out-of-plane ($\vec{\mathbf{E}}_{\perp}$) electric field vector components matter (see Fig. 1), and we shall simply speak of plane polarized x rays. They can be used to determine the direction of the out-of-plane magnetic axis. The NiO domain XMLD images are obtained by dividing two images taken at the two multiplet peaks comprising the Ni L_2-edge absorption spectra [8].

We use right or left circular polarization for x-ray magnetic *circular* dichroism (XMCD) experiments and the sign of the contrast depends on the handedness of the x rays [6]. The ferromagnetic Co XMCD images are obtained by dividing images taken at the L_2 and L_3 edges [4].

The NiO crystal was cleaved *ex situ* and immediately introduced into the ultrahigh vacuum PEEM2 instrument. The crystal was then annealed at 380 K for several hours to desorb contamination resulting from the short exposure to air. The low energy electron diffraction pattern of such crystals was characteristic of a well-ordered (001) surface. In a second step thin films (<2 nm) of Co or Fe were deposited onto the crystal. The base pressure in the UHV system was 5×10^{-10} torr. The deposition rate was about 0.04 nm per minute.

Above the Néel temperature ($T_N = 523$ K) the NiO lattice has a perfect fcc rocksalt structure. After cooling below T_N magnetoelastic forces cause a rhombohedral contraction of the crystal along different $\langle 111 \rangle$ axes and the crystallographic twinning leads to so-called *T*(win) domains. Within each *T* domain the spins lie in ferromagnetic $\{111\}$ planes, perpendicular to the contraction axes, with adjacent planes exhibiting antiferromagnetic alignment. Each *T* domain may furthermore split into three different *S*(pin) domains with spins along three possible directions, e.g., $[\bar{2}11]$, $[1\bar{2}1]$, and $[11\bar{2}]$ [9]. Within each *S* domain the crystal exhibits a triclinic distortion. Low energy domain walls between *T* domains correspond to the crystallographic *and* magnetic mirror planes $\{100\}$ and $\{110\}$. The magnetic axis in the wall is the average of those in the two adjacent *T* domains [10]. Examples of bulk *T* walls are shown in the lower panel of Fig. 2 as a green plane that separates two *T* domains, whose spin directions are also shown. The wall planes are mirror planes for both the magnetic and the crystallographic structures and the magnetic axes in the walls lie along [010] and [110], respectively.

Figure 2 shows an XPEEM image of the antiferromagnetic structure near the surface of cleaved NiO(001) using plane polarized x rays. Four different gray scales are observed, corresponding to antiferromagnetic domains with different spin orientations. A (100) wall separates domains exhibiting large contrast. They are further divided by (110) and $(\bar{1}10)$ walls into domains with weaker contrast. Local absorption spectra taken with either plane or linear polarization in each domain show that the magnetic axes in these domains are parallel to the $[\pm 1 \pm 2 \pm 1]$ directions. The in-plane orientations of the antiferromagnetic axes are indicated by the arrows in the image. Domains with the same in-plane orientation but different out-of-plane components can be distinguished because they have different projections on the out-of-plane component ($\vec{\mathbf{E}}_{\perp}$). In our analysis of the detailed spin orientation in the various domains we used a variety of images and spectra taken at different azimuthal orientations ϕ that will be published elsewhere [11].

At the bottom of Fig. 2 we illustrate a particularly important result which clearly demonstrates that the domain structure at the surface deviates from that in the bulk. Here we compare the observed spin directions for the case of (100) and (± 110) walls in bulk NiO to those observed at the NiO surface. Although the surface (± 110) walls observed by XPEEM are still crystallographic mirror planes they are no longer magnetic mirror planes, in contrast to (± 110) walls in the bulk. The observed surface (± 110) walls minimize the dipole and stray field energies at the surface by a compensated spin orientation perpendicular to the wall. In contrast, bulklike (± 110) walls would result in uncompensated surface spins, oriented parallel to the wall.

Figure 3 shows images taken after deposition of eight monolayers of Co onto the NiO surface. The left column shows antiferromagnetic and the right column ferromagnetic domain patterns. The upper two images were taken for the very same sample position as for Fig. 2, with the NiO image on the left taken with plane polarized x rays. The lower two images correspond to a different azimuthal orientation and the NiO image was taken with linear polarized x rays to enhance the contrast. Comparison of the top left image in Fig. 3 with that of the bare NiO surface in Fig. 2 reveals that after Co deposition the (± 110) walls disappear and only the (100) walls remain.

The ferromagnetic domains in the Co layer split up into two subgroups with each subgroup spatially following the

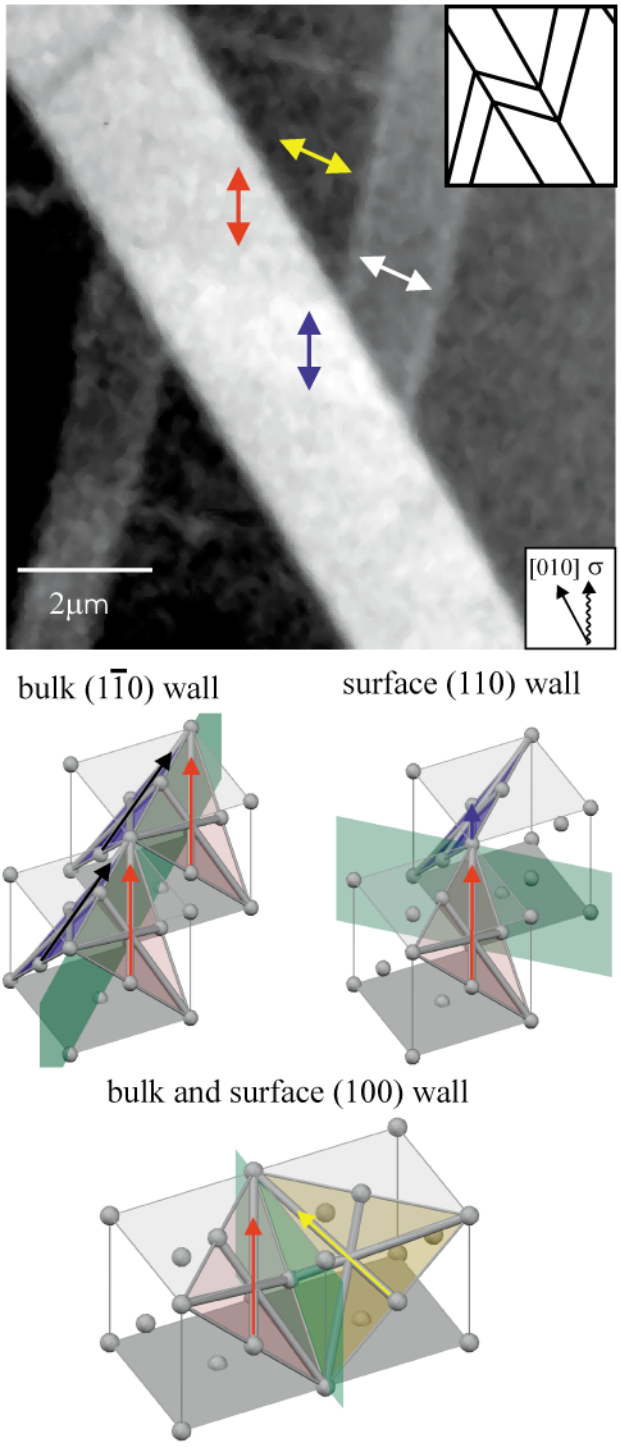

FIG. 2 (color). Antiferromagnetic domain structure of cleaved NiO(001) observed by XPEEM using plane polarization and an orientation $\phi = -30°$. Four different gray scales, representing four different antiferromagnetic domains are observed. The arrows indicate the in-plane projections of the antiferromagnetic axes which are [120] (red and blue) and [$\bar{1}$20] (white and yellow). Each in-plane axis splits up into two different out-of-plane axes. These are [121] (red), [12$\bar{1}$] (blue), [$\bar{1}$2$\bar{1}$] (yellow), and [$\bar{1}$21] (white). The inset in the upper right corner shows a sketch of the domain structure as a guide to the eye. Three type of domain walls (110), ($\bar{1}$10), and (100) can be identified. Models for typical domains and domain walls (green) for bulk NiO and for those observed by us near the cleaved surface are shown below.

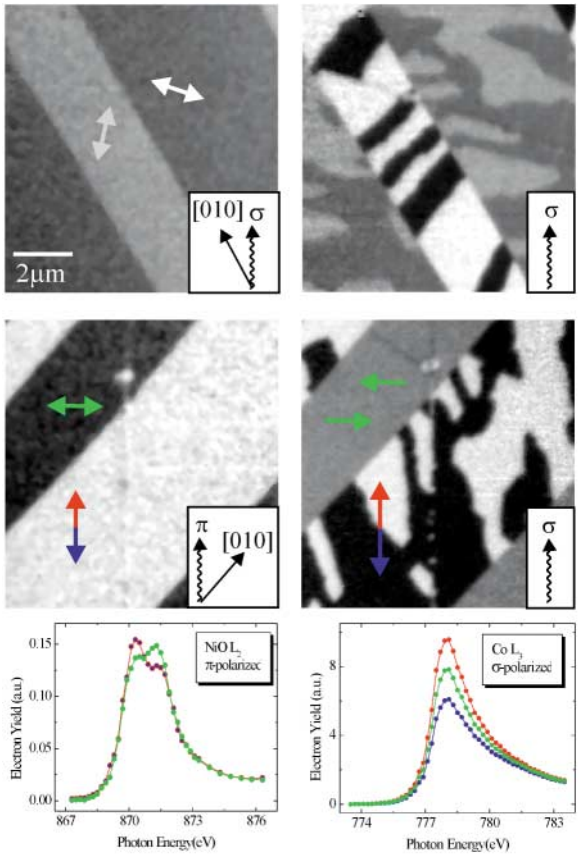

FIG. 3 (color). Comparison of antiferromagnetic (left column) and ferromagnetic (right column) domain patterns for eight monolayers of Co on NiO(001) and two different azimuthal geometries. Arrows and wavy lines indicate the directions of the magnetic axes and photon wave vectors, respectively. Linear polarization is labeled π, circular and plane polarization σ. Top panel: Same geometry as for Fig. 2 showing only half of the NiO domains. Each NiO domain has two corresponding Co domains with antiparallel spin alignment. Bottom panel: The sample is rotated so that $\vec{\mathbf{E}}_{\parallel} \parallel [110]$ ($\phi = 45°$). The contrast from one subgroup of ferromagnetic domains vanishes. The local spectra show the origin of the magnetic domain contrast.

antiferromagnetic domains. The observed spatial alignment of antiferromagnetic and ferromagnetic domains is caused by exchange coupling and it breaks up upon heating the system above the Néel temperature of NiO. In order to determine the orientation of the antiferromagnetic and ferromagnetic axes, the sample was azimuthally rotated and images and local spectra were taken for different geometries. For simplicity we show only the spectra taken with $\vec{\mathbf{E}}_{\parallel}$ parallel to [110] and the in-plane photon spin projection, parallel to [$\bar{1}$10] ($\phi = 45°$) in the lower row of Fig. 3. In this geometry the contrast from one subgroup of ferromagnetic domain vanishes, indicating that they are oriented perpendicular to [$\bar{1}$10]. The dichroism contrast of the other subgroup of ferromagnetic domains (black and white in lower right image) is about 30%, while the antiferromagnetic contrast in the lower left image is 14%. Both dichroism

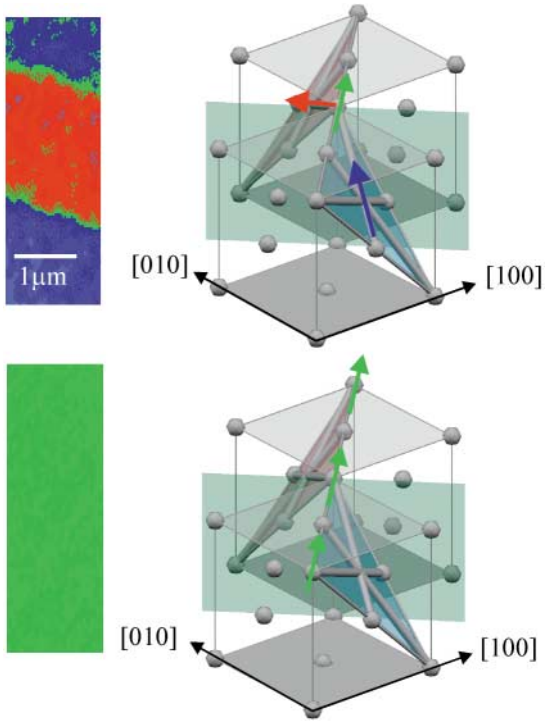

FIG. 4 (color). Illustration of the reorientation process of the antiferromagnetic axes at the surface of NiO(001) after deposition of Co. The observed domain structure for the bare crystal (top) and the coupled system (bottom) is compared to three-dimensional models on the right. The colors in the PEEM images correspond to those of the spin planes and axes in the models. The blue $(1\bar{1}1)$ and the red $(\bar{1}11)$ planes are separated by a (110) wall. After Co deposition all spins align along [110].

values are completely consistent with the maximum bulk values determined by Chen *et al.* [12] for Co and Alders *et al.* [7] for NiO, taking into account the different energy resolution in our experiment which affects the peak intensity. Because of the $1/e$ electron yield probing depth of about 2.5 nm [6] for both the Co and NiO layers, the observed domain structures arise from the entire Co layer, on one hand, and from more than the top ten layers of the NiO. Within this near-interface region of NiO the antiferromagnetic spin directions are completely in plane, parallel to $[\pm 110]$ and parallel to those in Co. Our orientational precision for the determination of the in-plane components is $\pm 5°$ and for the out-of-plane component $\pm 7°$.

Figure 4 illustrates the reorientation process in more detail. In the left column we show domain images taken before and after Co deposition at the same sample position. On the right we show the corresponding three-dimensional models of the structure and the spin orientation. The spin planes and axes are marked in corresponding colors. The top panel describes the results for the cleaved surface, already discussed in conjunction with Fig. 2. T domains with spin axes parallel to $[121]$ (dark blue) and $[12\bar{1}]$ (dark red) are separated by a (110) wall. The spin direction in the wall (green) is perpendicular to the wall, parallel to the common $[110]$ projection of both T domains. Upon Co deposition the (110) walls in the image vanish. Now all spins are parallel to $[110]$. The spins in the original T domains rotate by $\pm 30°$ in the (111)-like planes and align parallel to the surface, along $[110]$. All spins now lie in the (001) plane which is the spin configuration of a (001) wall parallel to the interface.

In summary, for the cleaved NiO(001) surface we observe only a subset of the bulk antiferromagnetic domains with formations of novel {110} domain walls. After Co deposition the antiferromagnetic spins reorient and align, domain by domain, parallel to the Co spin direction which is in plane. The antiferromagnetic NiO(001) surface resembles a NiO(001) wall parallel to the surface with fourfold domain symmetry about the surface normal. The Co layer itself assembles into ferromagnetic domains indicating a strong uniaxial anisotropy of the Co parallel to the antiferromagnetic axis. We observe the same behavior for Co and Fe deposition on the surface in the thickness range from 0.5–2 nm. The results are completely reproducible under the specified preparation conditions. Our results clearly demonstrate the sensitivity of the antiferromagnetic spin orientation to surface and interface effects. More generally, they point out that any realistic model for the magnetic exchange coupling at ferromagnetic-antiferromagnetic interfaces has to be based on the actual spin structure near the interface which may significantly deviate from that expected from the bulk.

[1] J. Nogués and I. K. Schuller, J. Magn. Magn. Mater. **192**, 203 (1999).
[2] A. E. Berkowitz and K. Takano, J. Magn. Magn. Mater. **200**, 552 (1999).
[3] H. Matsuyama, C. Haginoya, and K. Koike, Phys. Rev. Lett. **85**, 646 (2000).
[4] F. Nolting, A. Scholl, J. Stöhr, J. W. Seo, J. Fompeyrine, H. Siegwart, J.-P. Locquet, S. Anders, J. Lüning, E. E. Fullerton, M. F. Toney, M. R. Scheinfein, and H. A. Padmore, Nature (London) **405**, 767 (2000).
[5] S. Anders, H. A. Padmore, R. M. Duarte, T. Renner, T. Stammler, A. Scholl, M. R. Scheinfein, J. Stöhr, L. Séve, and B. Sinkovic, Rev. Sci. Instrum. **70**, 3973 (1999).
[6] J. Stöhr, H. A. Padmore, S. Anders, T. Stammler, and M. R. Scheinfein, Surf. Rev. Lett. **5**, 1297 (1998).
[7] D. Alders, L. H. Tjeng, F. C. Voogt, T. Hibma, G. A. Sawatzky, C. T. Chen, J. Vogel, M. Sacchi, and S. Iacobucci, Phys. Rev. B **57**, 11 623 (1998).
[8] J. Stöhr, A. Scholl, T. J. Regan, S. Anders, J. Lüning, M. R. Scheinfein, H. A. Padmore, and R. L. White, Phys. Rev. Lett. **83**, 1862 (1999).
[9] S. Saito, M. Miura, and K. Kurosawa, J. Phys. C **13**, 1513 (1980).
[10] W. L. Roth, J. Appl. Phys. **31**, 2000 (1960).
[11] H. Ohldag *et al.* (to be published).
[12] C. T. Chen, Y. U. Idzerda, H.-J. Lin, N. V. Smith, G. Meigs, E. Chaban, G. H. Ho, E. Pellegrin, and F. Sette, Phys. Rev. Lett. **75**, 152 (1995).